# Interaction of $Co_6$ cluster with γ-alumina surface: a quantum chemical study

*M. N. Mikhailov,[a]* G. M. Zhidomirov,[b] and A. Yu. Krylova[a]*

*[a]N. D. Zelinsky Institute of Organic Chemistry, Russian Academy of Sciences, 47 Leninskii prosp., 119991 Moscow, Russian Federation. Fax: +7 (495) 137 2935. E-mail: mik@ioc.ac.ru*
*[b]G. K. Boreskov Institute of Catalysis, Siberian Branch of the Russian Academy of Sciences, 5 prosp. Akad. Lavrent´eva, 630090 Novosibirsk, Russian Federation.*

The interaction of $Co_6$ cluster with partially dehydroxylated γ-alumina surface was studied by the DFT method. Hydrogen atoms of surface hydroxyl groups can be transferred to the metal particle to form partially oxidized cobalt states. The energy characteristics of hydrogen transfer were determined and changes in the electronic structure of supported $Co_6$ particles were characterized.

**Key words:** supported cobalt particles, surface hydroxyl groups of alumina, quantum chemical calculations.

Fine metal particles supported by various oxide supports are an important class of heterogenenous catalytic systems. They have found widespread applications in processing of hydrocarbons and in the synthesis of hydrocarbons from CO and $H_2$.[1]

The oxide surface serves not only as an inert support for the active component but can also affect its dispersity, electronic structure, chemisorption, and catalytic properties.[2,3] The circle of phenomena related to the metal—support interaction was termed as SMSI (Strong Metal—Support Interaction). One of the key structural features of the oxide support, which is responsible for the SMSI character, is the presence of hydroxyl groups on the oxide surface. A noticeable concentration of hydroxyl groups on the *in vacuo* heat-treated alumina surface is retained up to high temperatures (1000 K).[4]

Hydroxyl groups present on the oxide surface favor stabilization and high dispersity of the metal component and also affect the electronic structure of the supported particles.[5—8] Recently,[7] direct experimental evidence of the oxidation of supported rhodium nanoparticles by hydroxyl groups of alumina were obtained by photoelectron spectroscopy. Therefore, it was interesting to establish whether does this interaction manifest itself in the course of formation of oxidized metal particles in the $Co/Al_2O_3$ system. Interest in partially oxidized forms of the metallic component is due to a possible role of such forms in the Fischer—Tropsch process.[9,10] According to calculations of the interaction between metal particles and hydroxyl groups of the support, carried out for the $Rh_6$—H-form of faujasite system,[11] metal particles are oxidized by acidic hydroxyl groups of zeolite and hydroxyl protons are transferred to the metal surface (reverse spillover).

In this work, we chose the system comprising a $Co_6$ particle immobilized on γ-alumina surface as a simple model for active sites of cobalt catalysts of the Fischer—Tropsch synthesis. The main goal was to study the formation of partially oxidized particles and the mechanism of the interaction between cobalt particles and the surface hydroxyl groups of alumina.

## Calculation Procedure

Partially dehydroxylated alumina surface was described in the cluster approach. The electronic structures of clusters were calculated using the density functional theory (DFT) with the B3 exchange functional[12] and the LYP[13] and VWN5[14] (R-B3LYP) correlation functionals. In order to reduce the computing time, we used the SBKJC pseudopotential[15] and the corresponding basis set augmented with polarization functions on all atoms. All calculations were carried out using the GAMESS (US) program package.[16]

In studying the model for active γ-$Al_2O_3$ surfaces it was concluded that the most catalytically active face is the (110) face.[17] Correspondingly, the cluster simulating the surface of partially dehydroxylated alumina was assumed to have the structure of γ-$Al_2O_3$.[18] Since γ-$Al_2O_3$ has a defect spinel structure, the starting structure was chosen to be that of ideal spinel $MgAl_2O_4$, with the lattice constant corresponding to γ-$Al_2O_3$ ($a$ = 7.911 Å) with all Mg atoms replaced by Al atoms. To obtain a correct stoichiometry, certain Al atoms were removed leaving some cation positions vacant. Particular vacancy locations (*i.e.*, octahedral or

Published in Russian in *Izvestiya Akademii Nauk. Seriya Khimicheskaya,* No. 10, pp. 2194—2199, October, 2005.
1066-5285/05/5410-2264 

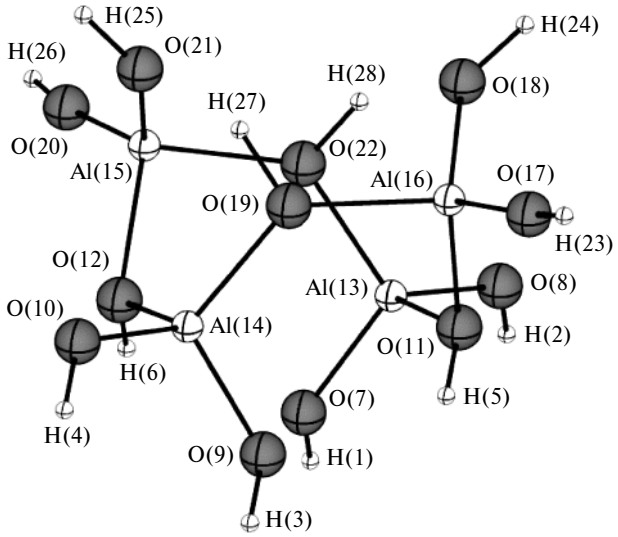


**Fig. 1.** Optimized structure of cluster simulating the surface of $\gamma$-$Al_2O_3$.

tetrahedral positions) are still to be clarified.[19,20] The model cluster represented a fragment of the (110) surface comprising four Al atoms bound to the surface O atoms.

Broken bonds of the cluster were saturated with hydrogen atoms placed at a distance of 0.96 Å from the O atoms along the lines of O—Al bonds in the crystal. To allow for the effect of support, all terminal OH groups, except for the surface hydroxyl groups, were fixed in the course of geometry optimization. The optimized structure of the cluster (cluster **1**) is shown in Fig. 1. The cluster contains two bridging surface hydroxyl groups (O(19)—H(27) and O(22)—H(28)), four terminal surface hydroxyl groups (O(17)—H(23), O(18)—H(24), O(20)—H(26), and O(21)—H(25)), and six fixed hydroxyl groups (from O(7)—H(1) to O(12)—H(6)). Under the catalyst preparation conditions[10] one can expect the formation of significantly dehydroxylated $\gamma$-$Al_2O_3$ surface. Such a surface can be simulated by removing one (cluster **1a**) or two (cluster **1b**) water molecules followed by geometry optimization for the clusters thus obtained (Fig. 2). Partially dehydroxylated $\gamma$-$Al_2O_3$ surface was simulated by cluster **1b** with two terminal hydroxyl groups O(17)—H(21) and O(19)—H(22).

An important problem in model calculations of transition-metal nanoclusters supported on oxide surfaces is the choice of the multiplicity of the metal particles under study. When using the total energy minimum criterion for free metal clusters, the optimum multiplicity strongly depends on the size (number of atoms) and shape of the cluster. For instance, the optimum multiplicity for a free $Co_6$ cluster is 15.[21] According to model calculations,[22] the interactions of the metal nanocluster with the adsorbate and support favor stabilization of low-spin states as in, *e.g.*, carbonyl complexes of cobalt clusters.[23] One can expect that treatment of a singlet $Co_6$ cluster provides a correct description of the interaction between the cobalt particle and the surface hydroxyl groups of alumina.

## Results and Discussion

Preliminary calculations showed that the interaction of the $Co_6$ cluster with partially dehydroxylated $\gamma$-$Al_2O_3$ surface involves a thermodynamically favorable transfer of protons of the surface hydroxyl groups of alumina to the surface of the $Co_6$ particle, accompanied by the formation of oxidized cobalt states.

The optimized geometric parameters of the clusters simulating the key intermediates and transition states of the interaction of the cobalt particle with partially dehydroxylated surface of alumina are shown in Fig. 3. Interaction between cluster **1b** and $Co_6$ nanoparticle is characterized by relatively high energy (3.95 eV) and results in an adsorption complex **2**. Adsorption involves four oxy-

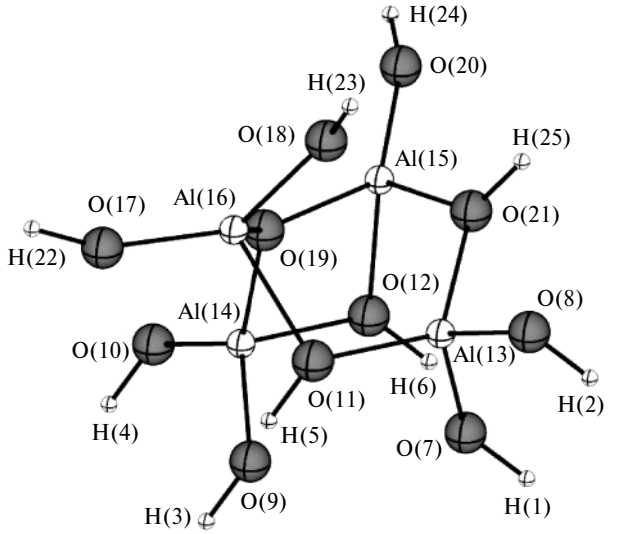


**1a**

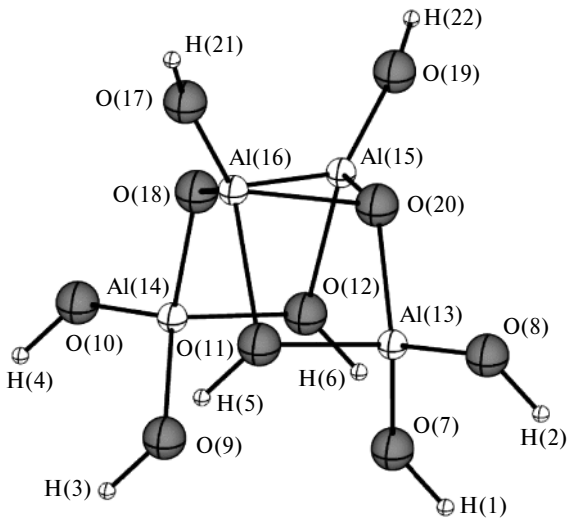


**1b**

**Fig. 2.** Optimized structures of clusters simulating the surface of partially dehydroxylated $\gamma$-$Al_2O_3$.

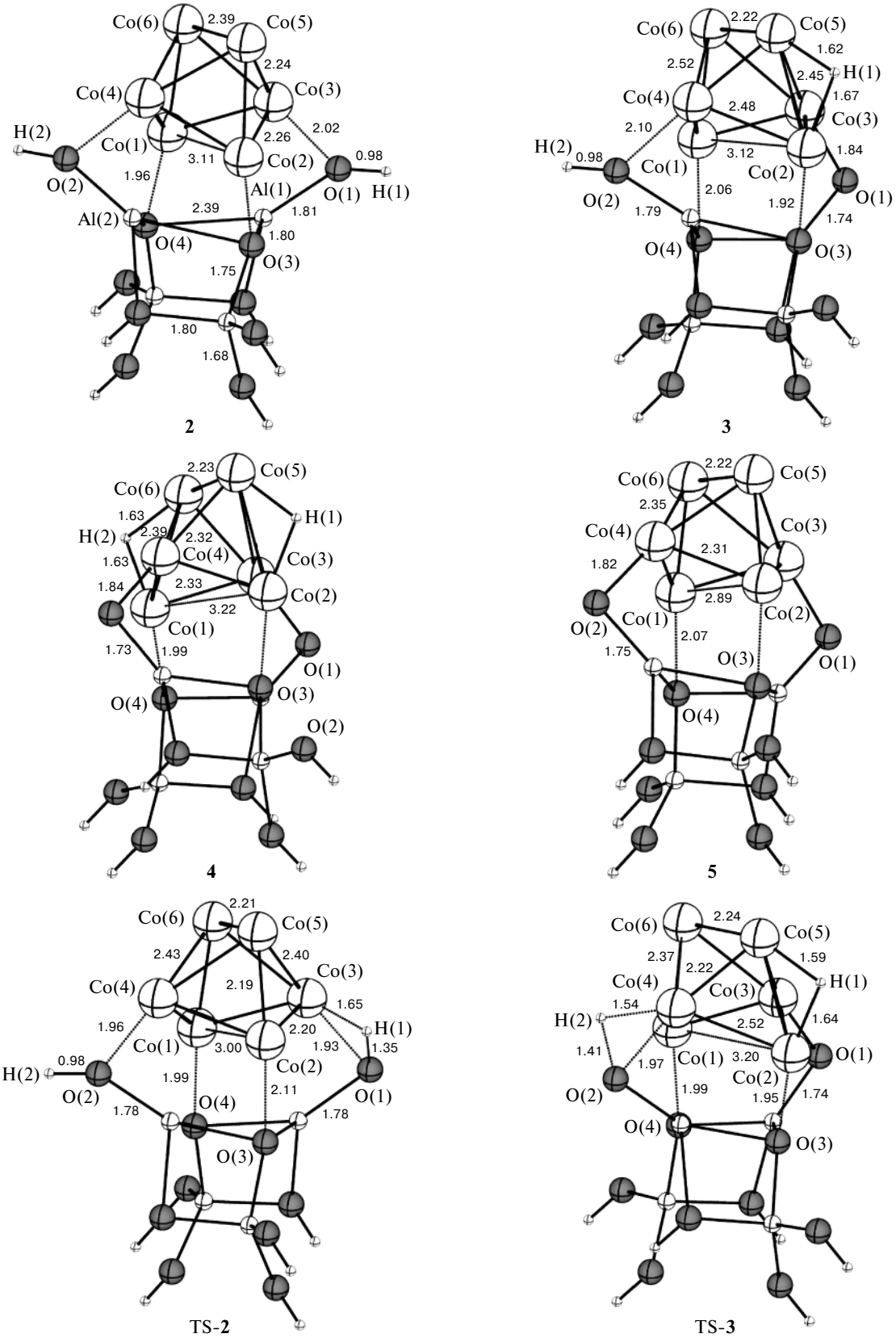


**Fig. 3.** Optimized structures of intermediates and transition states of proton transfer from the surface hydroxyl groups of $\gamma$-$Al_2O_3$ to $Co_6$ particle. The interatomic distances are given in Å.

gen atoms (two bridging and two hydroxyl oxygens) located at distances about 2.0 Å from the nearest cobalt atoms. As a result, the geometric parameters of the support and cobalt cluster are changed, namely, the Co(1)—Co(2) distance increased from 2.37 to 3.11 Å and the Al(1)—O(4) and Al(2)—O(3) distances from 1.95 to 2.39 Å. Other geometric parameters vary insignificantly.

Transfer of a hydroxyl proton to the surface of the metal particle through a transition state TS-**2** results in a surface structure **3**. In cluster **3**, the Co(3)—O(1) distance is decreased to 1.84 Å, and an adsorbed hydrogen state is formed at the Co(2)—Co(5) edge, with the 1.62 and 1.67 Å distances to cobalt atoms. Oxidized cobalt states are formed on the oxide surface. The charge of the metal particle in the structure with one transferred hydroxyl proton is 0.30. Transfer of the second surface hydroxyl proton involving the transition state TS-**3** leads to a surface cobalt cluster **4** with two adsorbed protons at the Co(2)—Co(5) and Co(1)—Co(6) edges; in this structure the charge of the metal particle increases to 0.45.

Proton transfer is an exothermic process ($\Delta E_1$ = −18 kcal mol$^{-1}$, $\Delta E_2$ = −12 kcal mol$^{-1}$) with activation energies $E_{a1}$ = 25 kcal mol$^{-1}$ and $E_{a2}$ = 28 kcal mol$^{-1}$, respectively (Fig. 4). The interaction of the $Co_6$ cluster with partially dehydroxylated surface of alumina involves transfer of protons of the surface hydroxyl groups to the metal particle, followed by the formation of oxidized cobalt states.

Further migration (spillover) of hydrogen across the surface of the metal particle followed by desorption to the gas phase can lead to structure **5**, thus resulting in the formation of mixed alumina—cobalt oxide fragments. In such structures, the charge of the $Co_6$ particle increases to a value of 0.57.

It was of interest to establish to which extent the energies of reactions and the activation barriers depend on,

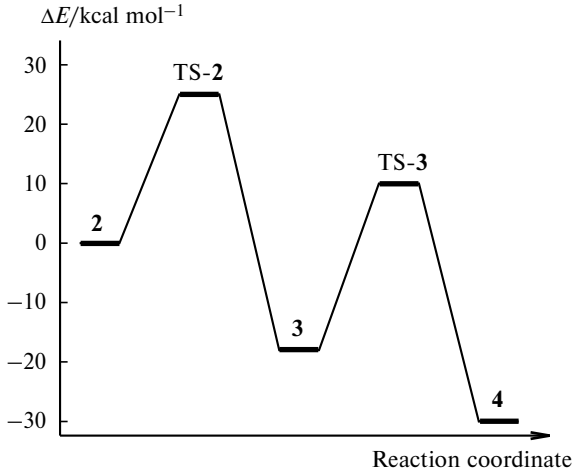


**Fig. 4.** Cross-section of potential energy surface for proton transfer from the surface hydroxyl groups of γ-$Al_2O_3$ to $Co_6$ particle.

**Table 1.** Energy characteristics of proton transfer from the surface hydroxyl groups to the metal particle in the $Co_4/(Al_2O_3)_2 \cdot 6H_2O$ and $Co_6/(Al_2O_3)_3 \cdot 5H_2O$ systems obtained from B3LYP/SBKJC calculations

| System | $\Delta E$ | $E_a$ |
|---|---|---|
| | kcal mol$^{-1}$ | |
| $Co_4/2Al_2O_3 \cdot 6H_2O$ | −19 | 29 |
| $Co_4/2Al_2O_3 \cdot 6H_2O$* | −21 | 28 |
| $Co_6/2Al_2O_3 \cdot 6H_2O$ | −18 | 25 |
| $Co_6/3Al_2O_3 \cdot 5H_2O$ | −15 | 24 |

* Obtained from B3LYP/SBKJC** calculations.

*e.g.*, the size of the support cluster, metal particle size, and extension of the basis set. The energy characteristics of proton transfer for a system with a large support cluster ($Co_6/(Al_2O_3)_3 \cdot 5H_2O$) and for a system containing a smaller cobalt particle ($Co_4/(Al_2O_3)_2 \cdot 6H_2O$) are listed in Table 1. According to calculations, changes in the sizes of both the metal particle and the support cluster have almost no effect on the energy characteristics of the process. Moreover, augmentation of the basis set with polarization functions on all atoms when calculating the second system, also causes no marked changes. Thus, the cluster chosen in this work seems to be sufficient for predictive description of the processes involving proton transfer from the surface hydroxyl groups to the cobalt particle followed by the formation of Co—O bonds.

The cluster structures **2—5** are strongly polarized. This follows from the results of atomic charge calculations for various cluster structures (Table 2). This is consistent with the published data.[11] Charge redistribution in the course of interaction between the $Co_6$ cluster and alumina surface is significant only for the surface hydroxyl group and

**Table 2.** Mulliken total atomic charges in clusters **2—5**

| Atom (cluster) | Charge, $q$/e | | | |
|---|---|---|---|---|
| | **2** | **3** | **4** | **5** |
| O(1) | −0.68 | −0.60 | −0.58 | −0.61 |
| O(2) | −0.69 | −0.69 | −0.56 | −0.55 |
| O(3) | −0.97 | −1.02 | −1.06 | −1.03 |
| O(4) | −0.98 | −1.06 | −1.09 | −1.08 |
| H(1) | 0.35 | 0.06 | 0.06 | — |
| H(2) | 0.35 | 0.35 | 0.08 | — |
| Co(1) | 0.37 | 0.62 | −0.03 | 0.82 |
| Co(2) | 0.36 | 0.16 | 0.08 | 0.71 |
| Co(3) | 0.13 | 0.15 | 0.43 | −0.31 |
| Co(4) | 0.15 | 0.00 | 0.39 | −0.38 |
| Co(5) | −0.48 | −0.35 | −0.25 | −0.12 |
| Co(6) | −0.46 | −0.34 | −0.31 | −0.15 |
| ($Co_6$) | 0.07 | 0.30* | 0.45* | 0.57 |

* With the charges of the transferred protons of hydroxyl groups.

the metal particle. Charge polarization in the initial metal particle (structure **2**) is characterized by large positive atomic changes of Co(1) and Co(2), nearest to the oxide surface. Additionally, positive charges on the intermediate atoms Co(3) and Co(4) decrease and the electron density is transferred to the Co(5) and Co(6) atoms in the upper layer of the metal cluster. The Co(6) atom remains almost neutral. An important feature of structure **3** with transferred proton is the charge redistribution (decrease in polarization) for the Co(2) and Co(5) atoms to which the adsorbed H atom is coordinated (see Fig. 3); this is accompanied by a marked increase in the positive charge of Co(1). A complex pattern of changes in polarization also manifests itself in the decrease in the absolute values of the atomic charges of Co(4) and Co(6). Transfer of the second proton (structure **4**) causes a considerable decrease in the charge polarization on the Co(1) and Co(6) atoms to which the second transferred proton is coordinated; the adsorbed H atoms remain virtually neutral. Transition to partially oxidized metal structure **5** leads to an appreciable increase in the positive atomic charges of Co(1) and Co(2) and negative atomic charges of Co(3) and Co(4).

The assumption of strong metal—support interaction with the formation of mixed oxide structures on the surface is also confirmed by the results of analysis of the densities of states and their changes due to immobilization of the metal particle on the oxide surface (Fig. 5). The interaction between the $Co_6$ cluster and the surface hydroxyl groups of alumina results in the shift of the oxygen 2p-levels by 0.8—1.5 eV toward higher binding energies and the appearance of cobalt d-lines on the right of the oxygen 2p valence levels in the band gap. As a result the band gap and ionization potential decrease by 4.24 and 3.02 eV, respectively (see Fig. 5a and Table 3, clusters **1b** and **2**). Proton transfer and subsequent formation of Co—O bonds leads to a shift of the cobalt d-bands toward higher binding energies, accompanied by an increase in the ionization potential and broadening of the band by 0.58 and 0.37 eV, respectively (see Fig. 5 and Table 3, clusters **2—4**). A chemical reaction occurs, which involves formation of oxidized cobalt particles and, correspondingly, stabilization of the metal cluster on the oxide surface. Similar changes were reported for catalysts on an acid support.[24] A study of the M—H resonance state observed in the XAFS spectra after adsorption of hydrogen revealed the reasons for changes in the electronic structure of supported metal particles.[25,26] In studying the adsorption of hydrogen on Pt particles supported on alumina it was found that an increase in the support acidity causes the Fermi level to shift toward higher binding energies and the energy difference ($E_{res}$) between the M—H antibonding state and the Fermi level to increase. Most likely, this effect appears to be characteristic of other transition-metal particles. In our case the support acidity increases on going from structure **3** to **4**. Correspondingly, the Fermi level is shifted by 0.44 eV toward higher binding energies. Positions of the Co—H antibonding states for structures **3** and **4** are arrowed in Fig. 5, *b*. The energy difference between the antibonding state Co—H and the Fermi level (HOMO) is 0.31 eV larger for structure **4** than for structure **3** (see Table 3), being consistent with the increase in the acidity of the support.

Thus, our DFT cluster calculations showed the possibility of exothermic transfer of hydrogen atoms from the

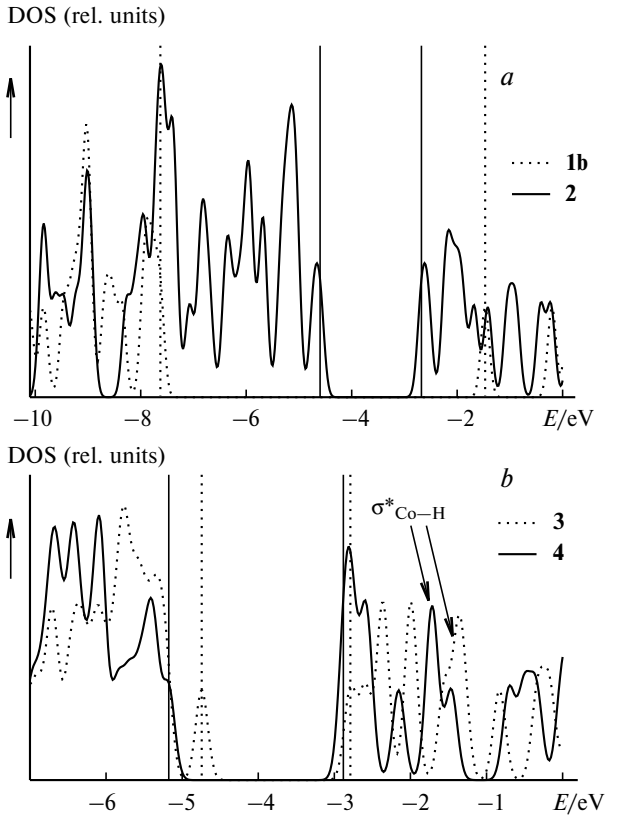


**Fig. 5.** Density of states (DOS) calculated for clusters **1b**, **2** (*a*) and **3**, **4** (*b*). Vertical lines denote the boundaries of the band gap (HOMO and LUMO).

**Table 3.** Energy characteristics of clusters **1b—5**

| Cluster | $IE^a$ | ε(LUMO) − ε(HOMO) | $E_{res}{}^b$ |
|---|---|---|---|
| | | eV | |
| **1b** | 7.62 | 6.16 | — |
| **2** | 4.60 | 1.92 | — |
| **3** | 4.74 | 1.96 | 3.18 |
| **4** | 5.18 | 2.29 | 3.49 |
| **5** | 5.13 | 2.26 | — |

[a] *IE* (ionization potential) = −ε(HOMO).
[b] $E_{res} = \varepsilon(\sigma^*_{Co-H}) - \varepsilon(LUMO)$.

surface hydroxyl groups of γ-alumina to the $Co_6$ particle, which results in the formation of partially oxidized cobalt states. The calculated changes in the d-states of cobalt particles are in agreement with experimental data for supported platinum particles.[24—26]

This work was financially supported in part by the Council on Grants at the President of the Russian Federation (Program for the State Support of Leading Scientific Schools in the Russian Federation, Project NSh 1140.2003.3 (G. M. Zhidomirov)).

## References

1. J. R. Anderson, *Structure of Metallic Catalyst*, Academic Press, New York, 1975.
2. *Metal-Support Interaction in Catalysis, Sintering, and Redispersion*, Eds. S. A. Stevenson, J. A. Dumesic, R. T. K. Baker, and E. Ruckenstein, Van Nostrand Reinhold, New York, 1987.
3. M. Che and C.O. Bennett, *Adv. Catal.*, 1989, **36**, 55.
4. J. B. Peri, *J. Phys. Chem.*, 1965, **69**, 220.
5. P. Basu, D. Panaytov, and J. T. Yates, Jr., *J. Am. Chem. Soc.*, 1988, **110**, 2074.
6. J. Libuda, M. Frank, A. Sandell, S. Andersson, P. A. Brühwiler, M. Bäumer, N. Mårtensson, and H.-J. Freund, *Surf. Sci.*, 1997, **384**, 106.
7. M. Heemeier, M. Frank, J. Libuda, K. Wolter, H. Kuhlenbeck, M. Bäumer, and H.-J. Freund, *Catal. Lett.*, 2000, **68**, 19.
8. M. Heemeier, S. Stempel, Sh. K. Shaikhutdinov, J. Libuda, M. Bäumer, R. J. Oldman, S. D. Jackson, and H.-J. Freund, *Surf. Sci.*, 2003, **523,** 103.
9. A. L. Lapidus and A. Yu. Krylova, *Usp. Khim.*, 1998, **67**, 1032 [*Russ. Chem. Rev.*, 1998, **67**, 941 (Engl. Transl.)].
10. P. Arnoldy and J. A. Moulijn, *J. Catal.*, 1985, **93**, 38.
11. G. N. Vayssilov, B. C. Gates, and N. Rösch, *Angew. Chem., Int. Ed. Engl.*, 2003, **42**, 1391.
12. A. D. Becke, *J. Chem. Phys.*, 1993, **98**, 5648.
13. C. Lee, W. Yang, and R. G. Parr, *Phys. Rev. B*, 1988, **37**, 785.
14. S. H. Vosko, L. Wilk, and M. Nusair, *Can. J. Phys.*, 1980, **58**, 1200.
15. W. J. Stevens, M. Krauss, H. Basch, and P. G. Jasien, *Can. J. Chem.*, 1992, **70**, 612.
16. M. W. Schmidt, K. K. Baldridge, J. A. Boatz, S. T. Elbert, M. S. Gordon, J. J. Jensen, S. Koseki, N. Matsunaga, K. A. Nguyen, S. Su, T. L. Windus, M. Dupuis, and J. A. Montgomery, *J. Comput. Chem.*, 1993, **14,** 1347.
17. O. Maresca, A. Allouche, J. P. Aycard, M. Rajzmann, S. Clemendot, and F. Hutschka, *J. Mol. Struct. (Theochem)*, 2000, **505**, 81.
18. E. J. W. Verwey, *Z. Kristallogr.*, 1935, **91**, 317.
19. K. Sohlberg, S. J. Pennycook, and S. T. Pantelides, *J. Am. Chem. Soc.*, 1999, **121**, 7493.
20. G. Gutierrez, A. Taga, and B. Johansson, *Phys. Rev. B*, 2001, **65**, 012101.
21. H.-J. Fan, C.-W. Liu, and M.-S. Liao, *Chem. Phys. Lett.*, 1997, **273**, 353.
22. R. V. Belosludov, S. Sakahara, K. Yajima, S. Takami, M. Kubo, and A. Miyamoto, *Appl. Surf. Sci.*, 2002, **189**, 245.
23. P. Macchi and A. Sironi, *Coord. Chem. Rev.*, 2003, **238/239**, 383.
24. D. C. Koningsberger, J. de Graaf, B. L. Mojet, D. E. Ramaker, and J. T. Miller, *Appl. Catal. A: Gen.*, 2000, **191**, 205.
25. D. C. Koningsberger, M. K. Oudenhuijzen, J. H. Bitter, and D. E. Ramaker, *Topics Catal.*, 2000, **10**, 167.
26. D. C. Koningsberger, D. E. Ramaker, J. T. Miller, J. de Graaf, and B. L. Mojet, *Topics Catal.*, 2001, **15**, 35.

*Received July 11, 2005;*
*in revised form August 29, 2005*